ELSEVIER

Microelectronic Engineering 61–62 (2002) 971–980

MICROELECTRONIC ENGINEERING

www.elsevier.com/locate/mee

Electrical properties of light-addressed sub-μm electrodes fabricated by use of nanostencil-technology

Volker Bucher[a,*], Jürgen Brugger[b,1], Dieter Kern[c], Gyu Man Kim[b,1], Markus Schubert[d], Wilfried Nisch[a]

[a]*Natural and Medical Sciences Institute, Markwiesenstrasse 55, D-72770 Reutlingen, Germany*
[b]*University of Twente, Nanolink, MESA + Research Institute, P.O. Box 217, NL-7500 AE Enschede, The Netherlands*
[c]*University of Tübingen, Institute of Applied Physics, Auf der Morgenstelle 10, D-72076 Tübingen, Germany*
[d]*University of Stuttgart, Institute of Physical Electronics, Pfaffenwaldring 47, D-70569 Stuttgart, Germany*

Abstract

A wide range of applications in neurotechnological research rely on planar microelectrode arrays (MEA) but the disadvantage of these systems is the low density of electrodes caused by the problem of wiring a great number of electrodes. In turn this results in a low number of good cell to electrode contacts. To overcome this drawback, a great number of laterally isolated sub-μm electrodes is placed on a photoconductor layer (amorphous silicon a-Si:H). By use of a laser beam, only those sub-μm electrodes lying under the cell can be selected to form an electrical contact to one of the underlying indium tin oxide (ITO) leads providing a high seal resistance at the cell/electrodes interface. A biocompatible and biostable composite layer of electrodes (100–500 nm) and insulator is formed using nanostencil-technology. Dark to bright ratio D of the photoconductor is determined to 10^5–10^6. The impedance of Au and TiN sub-μm electrodes in physiological solution is measured. Spatial resolution of the system is limited by light-scattering inside the supporting glass substrate; the effective diameter of the conductive region illuminated by the laser spot with intrinsic diameter 1.6 μm is ~6–7 μm.

Keywords: Sub-μm electrode chip; Light-addressing; Nanostencil; Shadow mask

1. Introduction

Microelectrode arrays (MEA) have been widely applied to study electrogenic cell cultures and tissue slices by extracellular recording and stimulation [1–4]. A microelectrode array based on thin

*Corresponding author. Tel.: +49-7121-5153-0856; fax: +49-7121-5155-3062.
E-mail address: bucher@nmi.de (V. Bucher).
[1]Present address: Ecole Polytechnique Fédérale de Lausanne (EPFL), Switzerland.

0167-9317/02/$ – see front matter
PII: S0167-9317(02)00422-7

film technology has the advantage of simultaneously measuring a large number of electrodes and thus a large number of cells [5,6]. However, caused by the problem of wiring a great number of electrodes, the disadvantage of these systems is the low density of electrodes which results in a low number of good cell–electrode contacts. Cells lying between the electrodes cannot be measured. In addition, cells usually do not adhere exactly on the electrode area. Thus each cell–electrode contact is different. As a consequence, the signal to noise ratio is not optimal and the signal cannot be detected properly. These problems can be solved using an array of light-addressable sub-μm electrodes providing a freely selectable cell–electrode contact with a high signal-to-noise ratio and high spatial resolution [7]. A great number of lateral isolated sub-μm electrodes is placed on a photo-conductor layer: hydrogenated amorphous silicon (a-Si:H). By use of a laser beam only those sub-μm electrodes lying under the cell can be selected forming an electrical contact to one of the underlying indium tin oxide (ITO)-leads and thus to an amplifier system providing a high seal resistance at the interface cell/electrodes (Fig. 1). The ensemble of all addressed sub-μm electrodes form a virtual microelectrode of some μm diameter. The smaller the sub-μm electrodes, the better the controlling of the position and shape of the formed virtual microelectrode (sampling theorem). Unfortunately, the photoconductor layer (a-Si:H) is not long-term stable in physiological solutions and has to be protected by a passivating layer.

In an earlier publication [8] we reported about the feasibility of fabricating a sub-μm electrode compound layer by use of electron beam lithography. This way of producing sub-μm electrodes is much too expensive for producing a measuring device. Thus we investigated the fabrication of sub-μm electrodes using nanostencil-technology [9]. These electrodes were contacted by a fine tungsten tip to determine the dark to bright ratio D of the resistance of sub-μm electrodes. Changing

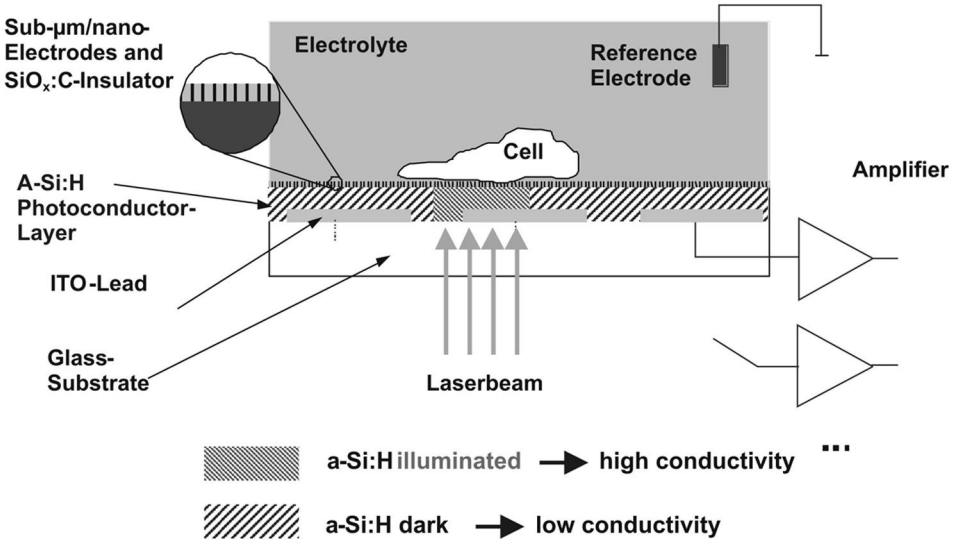

Fig. 1. Principle of light-addressed nano/sub-μm contacting of excitable cells. Electrodes over the illuminated photoconductor are switched through.

the position of the laser spot in the neighbourhood of the contacted electrodes gives information about the spatial resolution of the system.

2. Methods

2.1. Fabrication of light-addressable chip

A sputtered indium tin oxide (ITO) film (thickness $t_{ITO} = 150$ nm) on a glass substrate (49×49 mm^2, thickness $t_{glass} = 1$ mm) is structured in 60 parallel 1.8-mm-long rows each 20 μm wide with a distance of 10 μm to each other by standard photolithography and Ar plasma etching. Structuring the ITO is necessary because a photoconductor that is not illuminated provides a capacitance. Its shunt impedance would be too small if the ITO under the active area (1.8×1.8 mm^2) were not divided into rows, thereby increasing the shunt impedance to a value sufficient for a considerable signal to noise ratio. Each row is connected to one of the 60 contact pads at the edge of the glass substrate to allow for electrical connection to the amplifier. Amorphous silicon (a-Si:H) deposited as a 150-nm-thick film by plasma enhanced chemical vapor deposition (PECVD) technique serves as a photoconductor. Its absorbance of red laser light ($\lambda = 633$ nm) is 33%; for the case of blue laser light ($\lambda = 488$ nm) 95% is absorbed in the layer.

On top of the photoconductor, the sub-μm electrodes are structured using nanostencil-technology. Holes of diameter 300 nm and pitch of 1 μm are etched in an Si_3N_4 membrane of thickness 100 nm [10]. This microfabricated stencil serves as a shadow mask for evaporation (Fig. 2). Shadow mask evaporation is a method for depositing a metal pattern directly onto the substrate through a

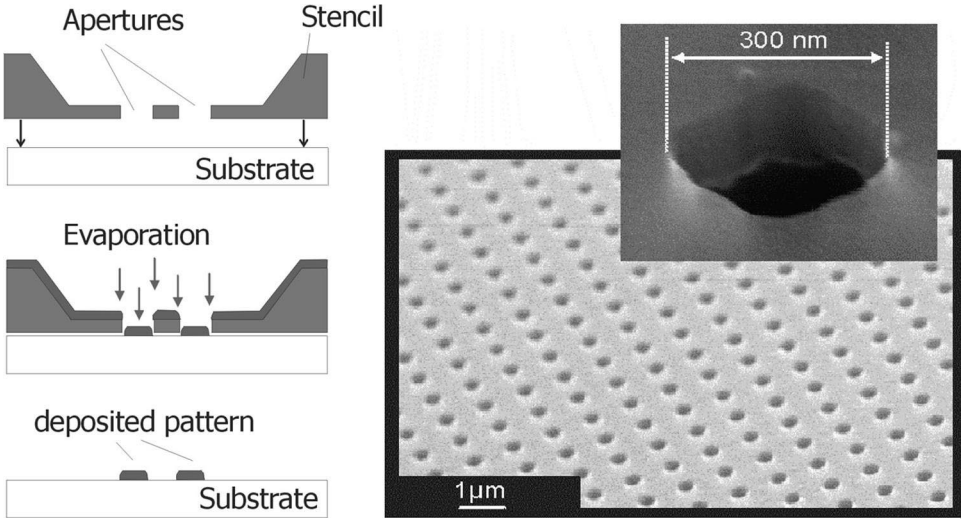

Fig. 2. Principle of nanostencil technique. Metal is evaporated through a shadow-mask with sub-μm apertures. The scanning electron image on the right side shows the mask used in this experiment.

microfabricated stencil without lithography steps. This low cost and simple resistless patterning process is intrinsically clean and can be applied to define metal patterns on arbitrary surfaces, e.g. also on organic layers, because it does not use any chemical solution during the process.

2.1.1. Fabrication of Au electrodes

On top of the a-Si:H, a thin Ti layer of 10 nm is deposited as an adhesion layer followed by a 650-nm-thick Au layer. Both materials were deposited using a Leybold Z550 sputtering machine. The vacuum pressure was 6×10^{-5} mbar. As a second step, 50-nm-thick Ti dots were patterned on top of the Au by evaporating Ti through the shadow mask in a Leybold L560 electron beam evaporation machine. This deposition was performed at a vacuum pressure of 6×10^{-5} mbar and a deposition rate of 1 nm/s. Ar plasma etching at a bias of 500 V (Leybold Z550, $t = 180$ min, $P_{HF} = 450$ W) led to cone shaped sub-μm electrodes with upper diameter 250 nm (Fig. 3). The step in the surface shown in the left part of Fig. 3 is caused by an ITO-bar of thickness 150 nm lying underneath the a-Si:H layer

2.1.2. Fabrication of TiN electrodes

Under high pressure (1.2×10^{-2} mbar) conditions sputtered TiN is an excellent biocompatible electrode material [11]. Typical impedance (at $f = 1$ kHz/$U = 100$ mV) of a 30 μm electrode in physiological saline solution is 30 kΩ. This TiN can be etched in a CF_4 plasma under bias. For fabrication of TiN sub-μm electrodes, three layers were deposited on top of the photoconductor (Fig. 4):

1. 300 nm Au with a 10-nm Ti adhesion layer (Leybold Z550);
2. 160 nm columnar TiN (Leybold L560);
3. 300 nm Au (Leybold Z550).

Again, 50-nm-thick Ti dots were patterned on top of the Au by evaporating Ti through the shadow

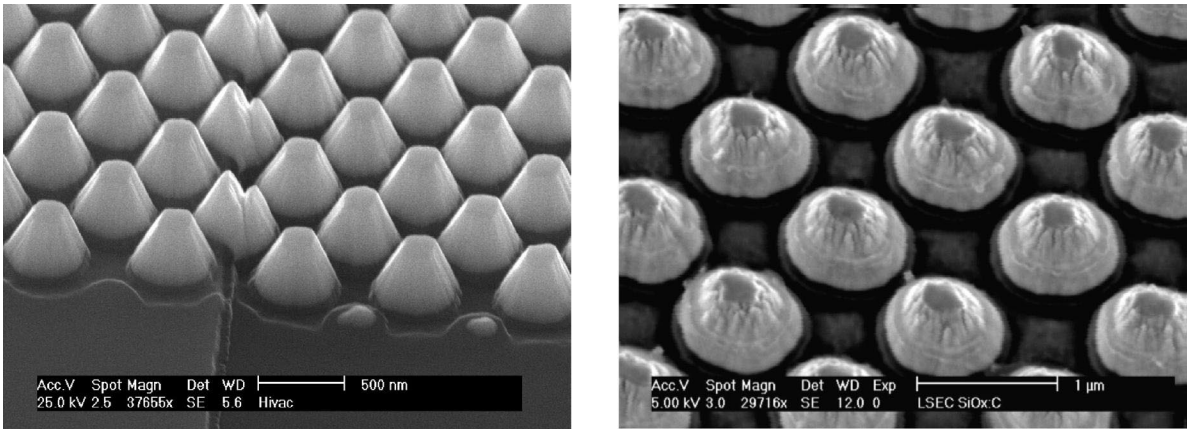

Fig. 3. Left, Au sub-μm electrodes fabricated by Ar plasma etching of a 650-nm-high Au layer patterned with Ti dots of diameter 250 nm. Right, high aspect Au sub-μm electrodes with passivated photoconductor. This scanning electron image was taken after removal of the levelling resist. The edge of the partially etched SiO_x:C insulator covering the photoconductor and the lower part of the electrodes can be seen clearly.

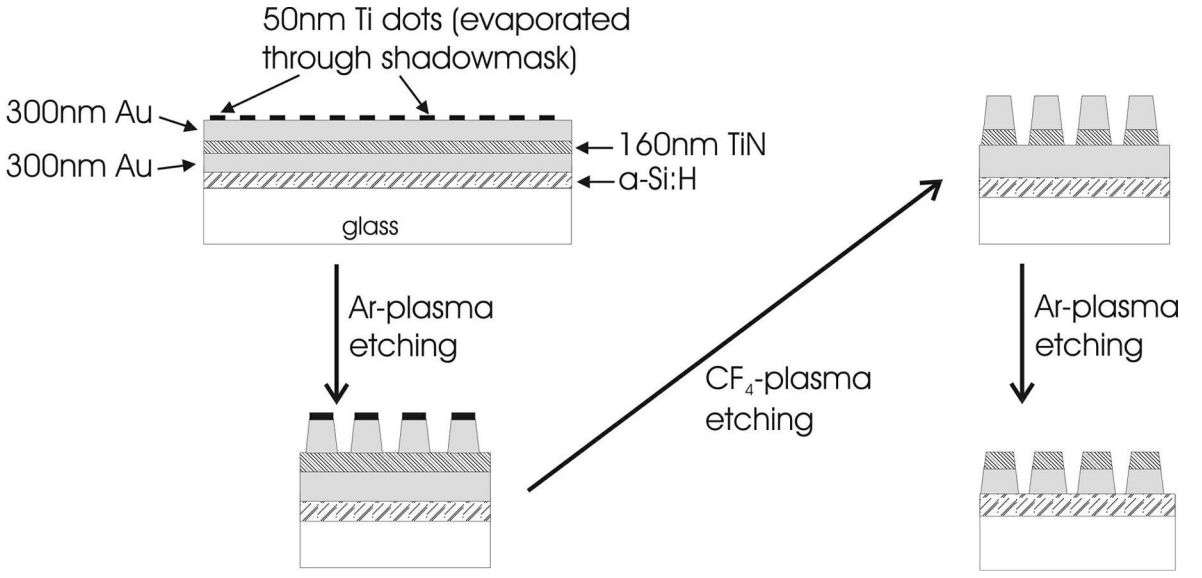

Fig. 4. Fabrication of columnar TiN sub-μm electrodes with high aspect ratio. The TiN layer is deposited by sputtering Ti in a high pressure Ar/N_2 plasma at 1.2×10^{-2} mbar.

mask. The upper Au layer with the Ti mask was etched in Ar plasma (Leybold Z550, $U = 500$ V, $t = 90$ min, $P_{HF} = 450$ W). The resulting Au cones serve as an etch mask when structuring the TiN in CF_4 plasma. This process removes the Ti dots, too. However, the underlying photoconductor, which also would be chemically etched in CF_4 plasma, still was protected by the first Au layer. The latter was structured in a second Ar plasma etching step removing the upper Au layer, too. In this way we got TiN sub-μm electrodes placed on Au cones.

2.1.3. The insulator layer

The photoconductor material (a-Si:H) is not stable in physiological solutions like physiological buffered saline solution (PBS). After some days in PBS at 37 °C it is diluted. For this reason, it has to be passivated between the electrodes. Because of the sub-μm dimensions, it is not feasible to align a second lithography mask. Thus we used a levelling technique.

A thin insulator layer (SiO_x:C) with a thickness of 25 nm for passivating a-Si:H was deposited over the electrodes by PECVD. Deposition was performed under 800 V bias in a PlasmaElectronic Piccolo machine. This layer has to be very thin to facilitate removal of the layer on top of the sub-μm electrodes. The electrode structure was levelled by deposition of Olin Hunt negative tone resist HNR80 (Fig. 5). After UV exposure and hardbake at 120 °C/$t = 1$ min on a hotplate the resist was partially etched in O_2 plasma in a PlasmaFab PECVD machine at $P_{HF} = 80$ W/$p = 450$ mTorr. Nine-minute etching led to electrodes—still covered with SiO_x:C—sticking out of the passivating layer. Etching in CF_4/O_2 plasma (90 sccm CF_4 + 10 sccm O_2 at pressure $p = 450$ mTorr) removed the passivating insulator over the freestanding part of the Au sub-μm electrodes. The right part of Fig. 3 shows the electrodes after removal of the HNR80 resist in Arch Chemical Microstrip remover. The edge of the insulator passivating the lower part of the electrodes and the a-Si:H can be seen clearly.

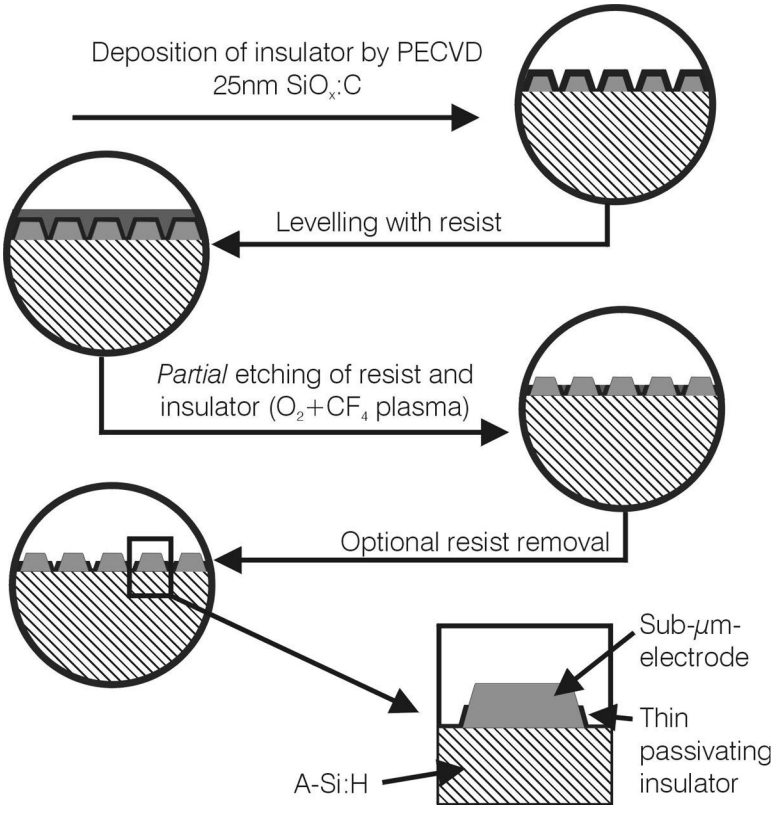

Fig. 5. Principle of passivating the photoconductor between the electrodes by levelling with photoresist.

Negative tone resist HNR80 itself could be used as passivating layer for short periods of exposure in physiological environment (some days). However, for long term studies, an SiO_x:C or Si_3N_4 insulator is necessary.

2.2. Determination of electrical properties

2.2.1. Dark to bright resistance ratio D of plasma-structured sub-μm electrodes

Earlier investigations showed that 150-nm-thick a-Si:H layers possess the best dark to bright resistance ratio ($D = 10^5$–10^6) when addressed with the blue Ar laser ($\lambda = 488$ nm, $P = 900$ μW) of a standard laser scan microscope (Zeiss LSM410, $10\times$-objective). These measurements were done using an intermediate light-addressable system with 3600 TiN electrodes of diameter 10 μm (MEC3600) [8,12]. Dark to bright resistance ratio D of sub-μm electrodes fabricated in the manner described above was determined by contacting them with a very thin tungsten tip. The radius of the tip was $r < 1$ μm, it was controlled using a Kleindiek Micromanipulator MM3. Measurements were done using a Zeiss LSM410 inverse laser scan microscope and a Keithley 236 DC Source Measure Unit. The position of the tip was monitored by help of an additional microscope mounted on top of the LSM410. Optical resolution of the additional microscope did not allow for contacting only one electrode. Caused by the diameter of the tip, an ensemble of ~4 sub-μm electrodes was contacted.

This was proved by measuring the imprint of the tip with higher resolution after the electrical measurements.

2.2.2. Dark to bright resistance ratio D of thin sub-μm electrodes fabricated without plasma etching

To avoid damaging the photoconductor as an effect of plasma etching, thin Au sub-μm electrodes were evaporated through the shadow mask onto the a-Si:H. Height of the electrodes was about 30 nm (10 nm Ti as adhesion promoter + 20 nm Au). Although these electrodes do not allow passivation of the a-Si:H, they can be used for measuring dark to bright resistance ratio D and spatial resolution of the system. Again, a thin tungsten tip ($r < 1$ μm) was used to contact the electrodes from above and an ensemble of ~4 electrodes was contacted.

2.2.3. Spatial resolution of the light-addressable system

The spatial resolution of the system can be determined when changing the position of the laser spot relative to the electrodes being contacted by the tungsten tip from above. Measurements with the intermediate test system MEC3600 published elsewhere [13] demonstrated that the resolution is limited by multiple reflection inside the 1-mm-thick glass substrate. Scattered light produces charge carriers in the vicinity of the main laser spot and partially switches through electrodes in the neighbourhood of the contacted sub-μm electrodes. By use of the 30-nm-high sub-μm electrodes, the spatial resolution can be determined with sub-μm resolution. An ensemble of ~4 sub-μm electrodes is contacted by the fine tungsten tip. The position of the laser spot was varied laterally to the contacted electrodes and DC resistance was monitored. Two different wavelengths ($\lambda = 488$ nm, $P = 800$ μW and $\lambda = 633$ nm, $P = 630$ μW) and a 10×-objective with numerical aperture of 0.3 were used; the diameter of the unscattered laser spot was determined to 1.6 ± 0.1 μm [13].

2.2.4. Impedance properties of the electrodes in physiological saline solution

To allow for sufficient signal to noise ratios, microelectrodes in physiological solutions (e.g. PBS) should have impedances smaller than 1 MΩ. Planar two-dimensional Au electrodes of diameter 10 μm are known to exhibit an impedance of 3–10 MΩ in PBS ($f = 1$ kHz). Calculating the impedance of flat sub-μm Au electrodes leads to values in the GΩ range. Consequently, Au should not be used as a material for two-dimensional sub-μm electrodes. On the other hand, fabrication of cone-shaped three-dimensional Au sub-μm electrodes using Ar plasma etching eventually could lead to smaller impedances caused by the three-dimensional geometry and surface roughening effects due to the ion bombardment. For this reason, Au electrodes were investigated, too. A TiN electrode of diameter 10 μm generally exhibits an impedance of 300 kΩ in PBS. Thus an ensemble on a circle of diameter 2–3 μm should show an impedance of 10–15 MΩ.

A Solartron SI1260 Gain Phase Analyser was used for AC measurements. The electrodes were covered with a negative tone resist pattern in the manner to define different sizes of electrically active sub-μm electrode ensembles (Fig. 6).

3. Results and discussion

DC current voltage traces of the plasma-etched sub-μm electrodes differ significantly from current voltage traces obtained by measurements with the intermediate light-addressable system MEC3600:

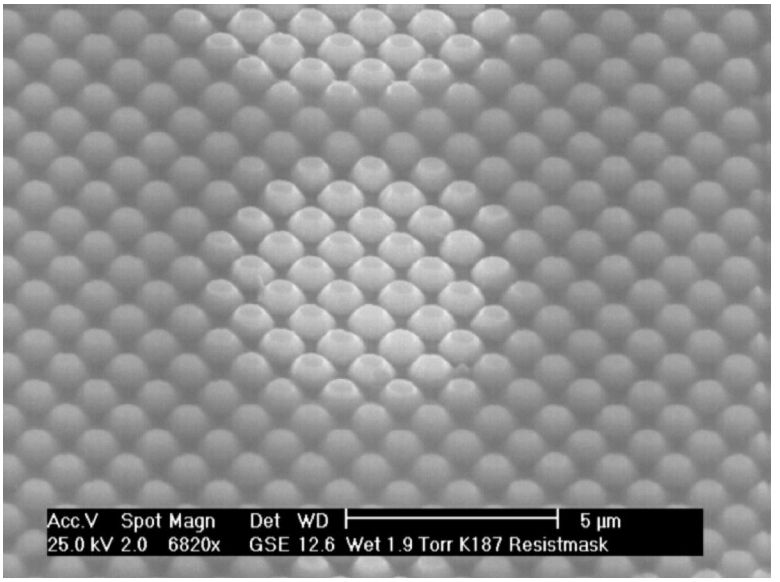

Fig. 6. Resist mask on sub-μm electrodes to define the size of the electrically active ensemble of electrodes. Diameters range from 2 μm up to 50 μm. Only the sub-μm electrodes in the open circle can contribute to current flow via the electrolyte.

electrodes of diameter 10 μm showed a dark resistance of $r=10^{9}$–10^{10} Ω. Under adequate laser illumination with a spot of diameter 1.6 μm a bright resistance of $r=10^{4}$ Ω could be achieved.

When measuring 650-nm-high Au sub-μm electrodes, only dark resistances of about 140 MΩ were measured. Illuminating the system with a red ($\lambda=633$ nm, $P=630$ μW) or a blue laser spot ($\lambda=488$ nm, $P=800$ μW) only decreased the resistance to ~60 MΩ. The drastic decrease of the dark to bright resistance ratio D from $D=10^{5}$–10^{6} to $D=2$ can be explained by damaging the photoconductor during the plasma etch process. Actually, the scanning electron image shown in the left part of Fig. 3 shows that the a-Si:H is also etched in the vicinity of sub-μm electrodes.

Resistance of directly evaporated thin sub-μm electrodes was determined to $r=10^{12}$–10^{13} Ω without illumination, a value already at the limit of the measurement set-up. Light-addressing the electrodes under the tip resulted in measured values between $r=390$–500 kΩ when using the blue laser ($\lambda=488$ nm, $P=800$ μW) and $r=1.0$–3.3 MΩ in the case of using the red laser ($\lambda=633$ nm, $P=630$ μW). The system shows the same dark to bright resistance ratio like 10-μm-electrodes of the intermediate system MEC3600.

The diffusion length of charge carriers in a-Si:H is ~10–100 nm [14] and does not have to be considered for affecting the spatial resolution of the system. Investigation of the conductivity under variation of laser power turned out that the correlation between photon density G and conductivity σ is almost linear: $\sigma \propto G^{0.88-0.95}$. No saturation effect at high photon densities ($G \approx 10^{25}$ s^{-1} cm^{-3}) could be found [13].

Fig. 7 shows the slope of the resistances when varying the position of the laser spot in a small range of a few μm. These measurements were done with the thin directly evaporated Au sub-μm electrodes. Minimal resistance is 390 kΩ in the case of the 488-nm-laser and 3.3 MΩ when using the

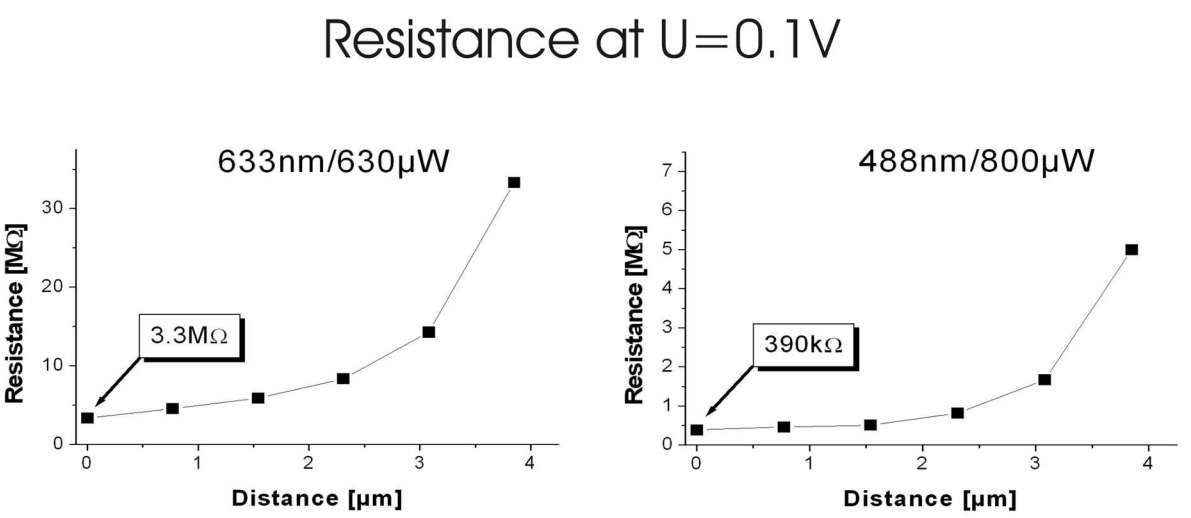

Fig. 7. Slope of the resistance of ~4 Au electrodes when varying the position of the laser spot in a small range of some μm. Minimal resistance is 390 kΩ in the case of the 488-nm-laser and 3.3 MΩ when using the 633-nm-laser.

633-nm-laser. Resistance increases for both wavelengths by a factor 10 when the lasers illuminate a point in 4 μm lateral distance from the tip. Conductivity and therefore photon density decreases down to 30% of the maximum value at distance 3.5 μm. When illuminating 30 μm away from the tip, resistance increases by approximately two orders of magnitude. The relevant conductive region, defined by photon densities bigger than 30% of the maximum value, can be determined to a circle of diameter 6–7 μm.

Impedance measurement of plasma etched Au and TiN sub-μm electrodes with passivated a-Si:H were done with a negative tone resist pattern (Fig. 6) in the manner to define different sizes of electrically active sub-μm electrode ensembles. It turned out that the impedance of Au electrodes is too big to allow a sufficient signal-to-noise ratio. Apparently no significant surface roughening occurred, thus Au electrodes cannot be used for the system. All measured impedances were in the range of some 10^7–10^8 Ω. These findings may be caused additionally by the damaging of a-Si:H during plasma etching.

However, measurements with sub-μm TiN electrodes on passivated a-Si:H showed an impedance of about 10 MΩ under illumination and 11–12 MΩ in darkness. A TiN electrode of diameter 10 μm generally exhibits an impedance of 300 kΩ in PBS. Thus an ensemble on a circle of diameter 2–3 μm should demonstrate an impedance of 10–15 MΩ. The measurement indicates that an ensemble on an illuminated circle of ~2.5–3 μm contributes to the impedance.

4. Conclusions and outlook

Feasibility of recording signals from excitable cells using the principle of light-addressing has been proven earlier [12] with the help of an intermediate system with 10-μm TiN electrodes (MEC3600) and a standard laser scan microscope (Zeiss LSM410).

In the present work, easy and economic fabrication of TiN and Au sub-μm electrodes embedded in

a passivating layer was established based on shadow evaporation through nanostencils. Columnar TiN electrodes exhibit an impedance small enough to be used in a light-addressable chip. The diameter of the addressing laser beam of a future system should be adapted to a diameter of 8–10 μm in order to achieve an impedance of 1 MΩ. This size of the addressed electrodes ensemble still would be small enough for contacting cells.

Fabrication of sub-μm electrodes with the high aspect ratio needed for passivating the a-Si:H between the electrodes required plasma etching. This step damages the electrical properties of the a-Si:H used as photoconductor. Thus the combination of a-Si:H and electrode/insulator compound layer described above cannot be used for a light-addressable sub-μm electrode chip. Further studies have to be done investigating other photoconductor materials which must not be protected against physiological solutions or establishing a well controllable wet-etching process for structuring the Au layer without any damaging of the underlying photoconductor.

Acknowledgements

This research was funded by the German Government under grant no. 0310964 A. The authors are grateful to Aquamarijn Micro Filtration B.V. for supplying the nanostencils. We thank Johnny Sanderink and Mark Smithers, MESA+/Uni Twente, for doing the evaporation experiments and SEM imaging, Doro Adam, IAP/Uni Tübingen for doing SEM imaging and Christiane Koehler, IPE/Uni Stuttgart for deposition of the photoconductors.

References

[1] J. Pine, M. Maher, S. Potter, Y.-C. Tai, S. Tatic-Lucic, J. Wright, in: Proceedings of the 18th Annual International Conference of the IEEE Engineering in Medicine and Biological Society, Vol. 5, 1997, pp. 2133–2135.
[2] J. Pine, J. Neurosci. Methods 2 (1980) 19.
[3] G.W. Gross, IEEE Trans. Biomed. Eng. 26 (1979) 273.
[4] J.B. Ranck Jr., in: M.M. Patterson, R.P. Kesner (Eds.), Electrical Stimulation Research Techniques, Academic Press, New York, 1981.
[5] A. Mohr, Dissertation an der Fakultaet fuer Chemie und Pharmazie der Eberhard-Karls-Universitat Tuebingen, 1995.
[6] W. Nisch et al., Biosens. Bioelectron. 9 (1994) 737.
[7] W. Nisch, Microelectrode arrangement, US Patent No. 6,032,062 (2000).
[8] V. Bucher, M. Schubert, D. Kern, W. Nisch, Microelectron. Eng. 57–58 (2001) 705–712.
[9] J. Brugger, J.W. Berenschot, S. Kuiper, W. Nijdam, B. Otter, M. Elwenspoek, Microelectron. Eng. 53 (2000) 403–405.
[10] C.J.M. van Rijn, G.J. Veldhuis, S. Kuiper, Nanotechnology 9 (1998) 343–345.
[11] M. Janders et al., in: 18th Annual International Conference of the IEEE Engineering in Medicine and Biological Society, Amsterdam, 1996.
[12] V. Bucher, B. Brunner, C. Leibrock, M. Schubert, W. Nisch, Biosens. Bioelectron. 16 (2001) 205–210.
[13] V. Bucher, Dissertation an der Fakultaet fuer Physik der Eberhard-Karls-Universitat Tuebingen, 2001.
[14] C.D. Abel, G.H. Bauer, Progress in Photovoltaics: Research and Applications Vol. 1 (1993) 269–278.